

Title	Synthesis of magnesium ZIF-8 from Mg(BH) .
Author(s)	Horike, S; Kadota, K; Itakura, T; Inukai, M; Kitagawa, S
Citation	Dalton transactions (2015), 44(34): 15107-15110
Issue Date	2015-04-01
URL	http://hdl.handle.net/2433/201994
Right	This journal is © The Royal Society of Chemistry 2015; The full-text file will be made open to the public on 1 April 2016 in accordance with publisher's 'Terms and Conditions for Self-Archiving'.
Type	Journal Article
Textversion	author

COMMUNICATION

Synthesis of magnesium ZIF-8 from $\text{Mg}(\text{BH}_4)_2$

Cite this: DOI: 10.1039/x0xx00000x

S. Horike,^{*a,b} K. Kadota,^a T. Itakura,^c M. Inukai,^d S. Kitagawa^{a,d}

Received 00th January 2012,

Accepted 00th January 2012

DOI: 10.1039/x0xx00000x

www.rsc.org/

Porous $\text{Mg}(\text{2-methyl imidazolate})_2$ (Mg-ZIF-8) was synthesised from $\text{Mg}(\text{BH}_4)_2$ as a precursor under an Ar atmosphere. It possesses an uncommon tetrahedral $\text{Mg}^{2+}\text{-N}$ coordination geometry that is stabilised by the formation of a framework, and it exhibits a Brunauer–Emmett–Teller surface area greater than $1800 \text{ m}^2 \text{ g}^{-1}$.

Porous coordination polymers (PCPs) or metal–organic frameworks (MOFs) that consist of metal ions and bridging ligands have been widely investigated for their possible applications in gas storage, separation and catalysis.^{1–3} Some properties of these materials are superior to those of conventional porous solids, and numerous attempts to adapt them to industrial applications have been reported.⁴ In view of applications, greater chemical and thermal stabilities are demanded, and several examples of stable MOFs with stable and inert coordination geometries have been reported.^{5,6} On the other hand, the construction of MOFs with uncommon coordination geometries is particularly challenging. The stabilization of such geometries by lattice formation has recently been investigated. For example, a tetrahedral $\text{Ni}^{2+}\text{-O}$ coordination geometry was successfully incorporated into a Zn^{2+} MOF by post-synthetic ion metathesis.⁷ In this case, the maximum doping ratio of the tetrahedral $\text{Ni}^{2+}\text{-O}$ centre in the framework was 25%, and the doping of Ni^{2+} beyond 25% led to a structural collapse. The stabilisation of uncommon coordination geometries in MOFs is fundamentally important in the area of coordination chemistry and for understanding catalytic reactions. Among a large variety of coordination modes, a tetrahedral $\text{Mg}^{2+}\text{-4X}$ ($X = \text{N}, \text{O}$, and so on.) coordination geometry is a rare example. The tetrahedral geometry in this case has $X\text{-Mg}^{2+}\text{-X}$ angles in the range of $105^\circ\text{--}115^\circ$ (ideal tetrahedral angle is 109.5°). According to the Cambridge Crystallographic Data Centre database, no crystal structure of a coordination polymer and an MOF having tetrahedral $\text{Mg}^{2+}\text{-N}$ and $\text{Mg}^{2+}\text{-O}$ coordination geometries is known. Only four crystal structures of discrete molecules with the tetrahedral $\text{Mg}^{2+}\text{-N}$ coordination geometry are known, and they all require bulky ligands.^{8–10} The literature contains five reports of the tetrahedral $\text{Mg}^{2+}\text{-O}$ coordination geometry, although many reports on distorted

four-coordinate Mg^{2+} compounds have been published. For these reasons, in this study, we aimed to stabilise the tetrahedral $\text{Mg}^{2+}\text{-N}$ coordination geometry in an MOF and characterise its structural stability and porosity.

Moreover, to construct an MOF with the tetrahedral $\text{Mg}^{2+}\text{-N}$ coordination geometry, we employed a well-known cubic structure, $[\text{Zn}(\text{2 mim})_2]$ (Figure 1, Zn-ZIF-8 , $\text{2 mimH} = \text{2-methyl imidazole}$) has a tetrahedral $\text{Zn}^{2+}\text{-N}$ coordination geometry and sodalite topology in its 3D extended structure.^{11,12} The $\text{N-Zn}^{2+}\text{-N}$ angle in the structure is 109.3° , and it exhibits a nondistorted, ideal tetrahedral coordination geometry. Zn-ZIF-8 has been widely studied in applications involving gas storage and separation because of its high porosity, high chemical stability and easy preparation. Co-ZIF-8 and Cd-ZIF-8 have been the isostructures of Zn-ZIF-8 .^{12–14} Isostructural zeolitic boron frameworks that contain tetrahedral Li-N and B-N have also been reported.¹⁵

We first attempted to synthesise the Mg^{2+} -based isostructure of Zn-ZIF-8 from anhydrous MgCl_2 under an Ar atmosphere. Several different combinations of synthesis conditions always provided a discrete complex $(\text{MgCl}_2(\text{2 mimH})_3)$.¹⁶ Chloride ions coordinate to Mg^{2+} centres to prevent the formation of a tetrahedral $\text{Mg}^{2+}\text{-N}$ core. To construct an MOF with an uncommon coordination geometry, we need to consider the reaction equilibrium because coordinating counter anions and solvents easily interrupt the formation of such geometry. On the basis of this idea, we used magnesium borohydride, $\text{Mg}(\text{BH}_4)_2$, as a starting reagent. In general, metal hydrides are reactive and are widely used as reductants in organic syntheses. Three tetrahedral $\text{Mg}^{2+}\text{-N}$ discrete complexes among the four reports described above are $\text{Mg}(\text{NH}_2\text{BH}_3)_4$ -based structures;^{9,10} this suggests that the tetrahedral $\text{Mg}^{2+}\text{-N}$ core preferentially forms in the presence of a hydride ligand. In the case of MOF construction, the reaction of $\text{Mg}(\text{BH}_4)_2$ and 2 mimH is expected to have H_2 gas as a by-product of an MOF construction, thereby promoting the formation of an extended structure. To the best of our knowledge, the literature contains only one report about the synthesis of an MOF from a metal hydride.¹⁷ In this previous report, BH_4^- anions from $\text{Mg}(\text{BH}_4)_2$ coordinate to Mg^{2+} to form a nonporous framework. Our synthesis was performed as follows: 10 mL of an acetonitrile solution of 2 mimH (82.1 mg, 100 mmol) was slowly added

dropwise to 10 mL of an acetonitrile solution of $\text{Mg}(\text{BH}_4)_2$ (27.0 mg, 50 mmol) at 298 K inside an Ar-filled glove box. Consequently, a white precipitate was generated when half of the ligand solution was added. The suspension was transferred to a hydrothermal bomb with a Teflon vial; the bomb was tightly sealed and heated at 373 K for 2 days. The white precipitate was filtered, and the powder was washed several times with acetonitrile and dried overnight at room temperature inside the glove box. We used two other concentrations for the reaction (2 mimH: $\text{Mg}(\text{BH}_4)_2 = 50:25, 150:75$ (mmol)), but they resulted in poorly crystalline compounds. We also used tetrahydrofuran as a synthesis solvent; this also resulted in the precipitation of poorly crystalline powders. The reactivity of $\text{Mg}(\text{BH}_4)_2$ precludes the use of protic solvents, and the optimisation of synthesis conditions is important to obtain a pure, highly crystalline compound.

and no decomposition or contamination was observed. Thus, we propose the reaction scheme as follows:



This reaction produces only gases as by-products, which is the key to obtaining phase-pure Mg-ZIF-8. Indeed, we monitored the bubbling of gases during the reaction of $\text{Mg}(\text{BH}_4)_2$ and ligand solutions. The final yield of Mg-ZIF-8 was 81% based on Mg^{2+} ions used, which is sufficiently high for MOF synthesis. In contrast to Zn-ZIF-8, Mg-ZIF-8 is quite sensitive to humidity in air. The results of our PXRD study indicate that Mg-ZIF-8 immediately decomposes when exposed to air. We obtained the PXRD patterns for Mg-ZIF-8 after the exposure for 10 min, and the pattern is identical to that for pure 2 mimH ligand. The 2 mim ligands coordinating to Mg^{2+} were exchanged for H_2O in air, and the released 2 mimH ligands recrystallised to form a bulk phase. This moisture sensitivity indicates that the chemical stability of Mg-ZIF-8 is not high. Because of the high air-reactivity of Mg-ZIF-8, we could not analyse it by thermogravimetric analysis. Differential scanning calorimetry was feasible under an Ar atmosphere, and the resulting trace did not show any peak in the temperature range of 298 K–473 K, suggesting that no phase transition or decomposition occurs in this temperature region. Thus, the thermal stability of Mg-ZIF-8 is sufficient to evaluate gas adsorption properties.

On the basis of the previously discussed results, we activated the powder sample of Mg-ZIF-8 at 353 K under vacuum for 12 h to remove all adsorbed solvents. The PXRD pattern of the activated powder under an Ar atmosphere is identical to that of the as-prepared sample. Figure 2 shows the N_2 and CO_2 adsorption and desorption isotherms for Mg-ZIF-8 and Zn-ZIF-8. None of the sorption isotherms exhibit hysteresis, and all exhibit Type-I profiles; this adsorption behaviour is typical of microporous solids (i.e. those with pore diameters less than 2 nm).¹⁸ The amount of N_2 adsorbed at 77 K for Mg-ZIF-8 was 589 mL g^{-1} at 100 kPa, which is higher than that adsorbed by Zn-ZIF-8 (410 mL g^{-1}). The Brunauer–Emmett–Teller (BET) surface area of Mg-ZIF-8 was 1806 $\text{m}^2 \text{g}^{-1}$, whereas that of Zn-ZIF-8 was 1660 $\text{m}^2 \text{g}^{-1}$. The amount of CO_2 adsorbed at 195 K by Mg-ZIF-8 was higher than adsorbed by Zn-ZIF-8, reaching 322 mL g^{-1} at 99 kPa. The formula weights of Zn-ZIF-8 and Mg-ZIF-8 are 229.60 and 188.53 g mol^{-1} , respectively, and the higher BET surface area of Mg-ZIF-8 is because of its lower molecular weight and larger cell volume than Zn-ZIF-8; i.e. the guest-accessible pore spaces of Zn-ZIF-8 and Mg-ZIF-8 are similar. The N_2 and CO_2 adsorption isotherms for Zn-ZIF-8 show a plateau above 30 kPa, whereas those of Mg-ZIF-8 show a gradual increase of gas uptake even at a pressure above 30 kPa. The PXRD pattern of the Mg-ZIF-8 sample under an Ar atmosphere after these gas-adsorption measurements was the same as that obtained before the sample was subjected to the isotherm measurements, indicating that the original porous structure of Mg-ZIF-8 remained intact after the gases adsorptions. At this stage we do not have direct evidence about the presence of hydride species inside the product, and further characterization such as solid state ^1H NMR would be helpful.

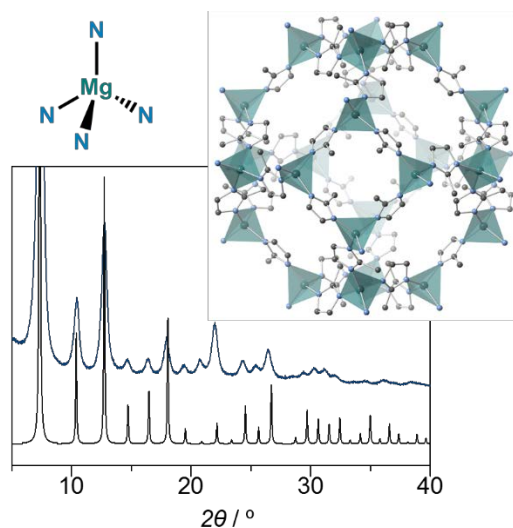


Figure 1. Powder X-ray diffraction pattern of Mg-ZIF-8 (blue) under an Ar atmosphere and the pattern of Zn-ZIF-8 simulated from its single-crystal structure (black). The crystal structure of Zn-ZIF-8 and the tetrahedral Mg^{2+} -N coordination geometry are also shown.

Figure 1 shows the powder X-ray diffraction (PXRD) pattern of the synthesised powder product; this pattern was obtained with the product under an Ar atmosphere. A simulated PXRD pattern of Zn-ZIF-8 is also shown. All diffraction peaks of the product in the 2θ range of 5° – 35° match those of Zn-ZIF-8; this suggests that the product has the same topology as Zn-ZIF-8. Hereafter, we denote the product as Mg-ZIF-8. The broad peaks are because of the adsorption of X-ray by Argon atmosphere, and probably small particle size of the product, though it is impossible to observe them by scanning electron microscope. We determined the space group and cell parameters of the product on the basis of the PXRD data, i.e. the product crystallised in the same space group ($I-43m$) as Zn-ZIF-8, with a lattice parameter of $a = 17.28(5)$ Å. This space group suggests that Mg-ZIF-8 possesses a nondistorted tetrahedral Mg^{2+} -N coordination geometry. The unit-cell parameter of Zn-ZIF-8 at 298 K is $a = 17.01$ Å, as calculated from the PXRD data of synthesised degassed Zn-ZIF-8, which indicates that the volume of the unit cell for Mg-ZIF-8 (5159.8 Å³) is 5% larger than that of Zn-ZIF-8 (4921.7 Å³). We attempted to obtain the single-crystal structure of Mg-ZIF-8; however, we were unsuccessful. To determine the composition of Mg-ZIF-8, we degraded the dried sample and obtained its ^1H -NMR spectrum. The spectrum exhibits only peaks of the 2 mimH ligand,

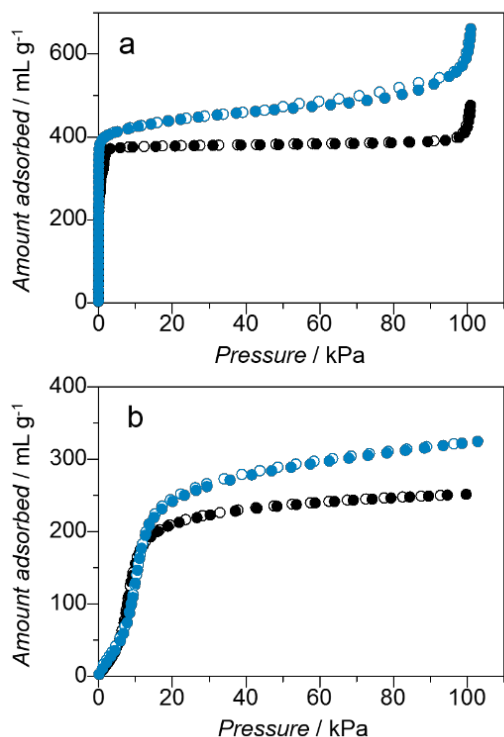


Figure 2. Adsorption (solid circles) and desorption (open circles) of Mg-ZIF-8 (blue) and Zn-ZIF-8 (black) for (a) N₂ at 77 K and (b) CO₂ at 195 K.

In this study, the formation of the framework of Mg-ZIF-8 was demonstrated to significantly stabilise the tetrahedral Mg²⁺-N coordination geometry. We estimated the energies of the lattice formations of Zn-ZIF-8 and Mg-ZIF-8 using *ab initio* calculations, as implemented in the DMol code.¹⁹ Total energy calculations were performed for a periodic cell at the DFT/PBE level.²⁰ Compared with the coordination bond of Zn²⁺-N in Zn-ZIF-8, the energy of the coordination bond of Mg²⁺-N in Mg-ZIF-8 is 138 kJ mol⁻¹ lower. This instability is thermodynamically substantial, and the ability of such a small lattice formation energy to preserve the highly porous framework is surprising. The charge analysis results revealed that more electrons transfer from 2 mim to Zn²⁺ via coordination bond formation in Zn-ZIF-8, indicating that the Zn²⁺-N bond exhibits a greater degree of covalent character than the Mg²⁺-N bond. However, in the case of Mg-ZIF-8, the charge on Mg²⁺ is more positive; thus, the nature of the Mg²⁺-N bond is more ionic. These calculation results suggest that the nature of the metal-N bonding in these compounds fundamentally differs.

Conclusions

We synthesised an Mg²⁺-ion-based zeolitic imidazolate framework, Mg-ZIF-8, with an uncommon tetrahedral Mg²⁺-N coordination geometry. The synthesis was made feasible by using Mg(BH₄)₂ as a starting reagent, and the resultant framework possesses permanent porosity, with a BET surface area greater than 1800 m² g⁻¹. This study demonstrates the potential of synthesising unique MOFs from various metal hydrides. Our stabilisation and characterisation of the uncommon coordination geometry of Mg²⁺ inside an MOF contributes to the fundamental advancement of coordination chemistry and to understanding of catalytic reactions.

This work was supported by a Grant-in-Aid for Young Scientists (A) and a Grant-in-Aid for Scientific Research on the Innovative Areas: 'Fusion Materials' from the Ministry of Education, Culture, Sports, Science and Technology, Japan and the PRESTO program of the Japan Science and Technology Agency (JST).

Notes and references

^a Department of Synthetic Chemistry and Biological Chemistry, Graduate School of Engineering, Kyoto University, Katsura, Nishikyō-ku, Kyoto 615-8510, Japan

^b Japan Science and Technology Agency, PRESTO, 4-1-8 Honcho, Kawaguchi, Saitama 332-0012, Japan

^c DENSO CORPORATION, 1-1 Showa-cho, Kariya, Aichi 448-8661, Japan

^d Institute for Integrated Cell-Material Sciences (WPI-iCeMS), Kyoto University, Yoshida, Sakyo-ku, Kyoto 606-8501, Japan

† Electronic Supplementary Information (ESI) available: [Experimental procedures, PXRD, DSC]. See DOI: 10.1039/c000000x/

1. M. Eddaoudi, D. B. Moler, H. Li, B. Chen, T. M. Reineke, M. O'Keeffe and O. M. Yaghi, *Acc. Chem. Res.*, 2001, 34, 319-330.
2. S. Kitagawa, R. Kitaura and S. Noro, *Angew. Chem. Int. Ed.*, 2004, 43, 2334-2375.
3. H. C. Zhou, J. R. Long and O. M. Yaghi, *Chem. Rev.*, 2012, 112, 673-674.
4. A. U. Czaja, N. Trukhan and U. Muller, *Chem. Soc. Rev.*, 2009, 38, 1284-1293.
5. G. Férey, C. Mellot-Draznieks, C. Serre, F. Millange, J. Dutour, S. Surble and I. Margiolaki, *Science*, 2005, 309, 2040-2042.
6. J. H. Cavka, S. Jakobsen, U. Olsbye, N. Guillou, C. Lamberti, S. Bordiga and K. P. Lillerud, *J. Am. Chem. Soc.*, 2008, 130, 13850-13851.
7. C. K. Brozek and M. Dincă, *Chem. Sci.*, 2012, 3, 2110.
8. T. Y. Her, C. C. Chang and L. K. Liu, *Inorg. Chem.*, 1992, 31, 2291-2294.
9. H. Wu, W. Zhou, F. E. Pinkerton, M. S. Meyer, Q. Yao, S. Gadipelli, T. J. Udovic, T. Yildirim and J. J. Rush, *Chem. Commun.*, 2011, 47, 4102-4104.
10. Y. S. Chua, W. Li, G. T. Wu, Z. T. Xiong and P. Chen, *Chem. Mater.*, 2012, 24, 3574-3581.
11. X. C. Huang, Y. Y. Lin, J. P. Zhang and X. M. Chen, *Angew. Chem. Int. Ed.*, 2006, 45, 1557-1559.
12. K. S. Park, Z. Ni, A. P. Côté, J. Y. Choi, R. Huang, F. J. Uribe-Romo, H. K. Chae, M. O'Keeffe and O. M. Yaghi, *Proceedings of the National Academy of Sciences*, 2006, 103, 10186-10191.
13. R. Banerjee, A. Phan, B. Wang, C. Knobler, H. Furukawa, M. O'Keeffe and O. M. Yaghi, *Science*, 2008, 319, 939-943.
14. Y. Q. Tian, S. Y. Yao, D. Gu, K. H. Cui, D. W. Guo, G. Zhang, Z. X. Chen and D. Y. Zhao, *Chem. Eur. J.*, 2010, 16, 1137-1141.
15. J. Zhang, T. Wu, C. Zhou, S. Chen, P. Feng and X. Bu, *Angew. Chem. Int. Ed.*, 2009, 48, 2542-2545.
16. F. L. Phillips, F. M. Shreeve and A. C. Skapski, *Acta Crystallographica Section B Structural Crystallography and Crystal Chemistry*, 1976, 32, 687-692.
17. M. J. Ingleson, J. P. Barrio, J. Bacsá, A. Steiner, G. R. Darling, J. T. Jones, Y. Z. Khimyak and M. J. Rosseinsky, *Angew. Chem. Int. Ed.*, 2009, 48, 2012-2016.
18. K. S. W. Sing, *Pure Appl. Chem.*, 1982, 54.
19. B. Delley, *J. Chem. Phys.*, 1990, 92, 508.
20. J. P. Perdew, K. Burke and M. Ernzerhof, *Phys. Rev. Lett.*, 1996, 77, 3865-3868.

